Journal of Pharmaceutical Sciences 108 (2019) 1964-1972

Contents lists available at ScienceDirect

Journal of Pharmaceutical Sciences

journal homepage: www.jpharmsci.org

Pharmaceutical Biotechnology

Rapid Prediction of Deamidation Rates of Proteins to Assess Their Long-Term Stability Using Hydrogen Exchange–Mass Spectrometry

Chamalee L.D. Gamage [1], Tyler S. Hageman [1], David D. Weis [1, 2, *]

[1] Department of Chemistry, The Ralph N. Adams Institute for Bioanalytical Chemistry, The University of Kansas, 1567 Irving Hill Road, Lawrence, Kansas 66045

[2] Department of Pharmaceutical Chemistry, The University of Kansas, 1567 Irving Hill Road, Lawrence, Kansas 66045

ARTICLE INFO

Article history:
Received 24 October 2018
Revised 14 January 2019
Accepted 17 January 2019
Available online 23 January 2019

Keywords:
deamidation
deuterium exchange
mass spectrometry (MS)
protein (s)
stability

ABSTRACT

Deamidation is an important degradation pathway for proteins. Estimating deamidation propensities is essential for predicting their long-term stability. However, predicting deamidation rates in folded proteins is challenging because higher-order structure has a significant and unpredictable effect on deamidation. Here, we investigated the correlation between amide hydrogen exchange (HX) and deamidation to assess the potential of using hydrogen exchange–mass spectrometry (HX-MS) to rapidly predict deamidation propensity. Maltose-binding protein and a structurally less stable mutant, W169G, were stored in the dark at pH 7.0 at 23 ± 2°C for 1 year. Deamidation at each asparagine site was measured using liquid chromatography–mass spectrometry after trypsin digestion. Deamidation rates at each deamidation site were determined based on first-order kinetics. HX rates at the deamidation sites were determined before storage using the shortest peptic peptide containing each site using conventional bottom-up HX-MS at pD 7.0 at 25°C. We observed a power law correlation between deamidation half-life and HX half-life for the NG sites with measurable kinetics. For NA sites, slow deamidation was only observed at 2 sites located in rapidly exchanging regions. Our findings demonstrate that HX-MS can be used to reliably and rapidly rank deamidation propensity in folded proteins.

Introduction

Proteins are increasingly used as therapeutics to treat various diseases because of their safety and efficacy.[1-7] However, proteins are susceptible to a variety of modifications during expression, purification, formulation, and long-term storage, potentially leading to loss of efficacy or a decrease in safety.[8,9] Among various protein modifications, deamidation is one of the most common degradation reactions, occurring during production and long-term storage. Deamidation (see Scheme 1) is a spontaneous, post-translational modification in which asparagine converts to aspartate or isoaspartate and glutamine coverts to glutamate.[10-13] This conversion introduces a negatively charged side chain and increases the mass of the protein by 0.984 Da. Furthermore, formation of isoaspartate alters the protein backbone by inserting a methylene group.[14] These modifications cause charge, size, and structural heterogeneity in proteins that can alter protein conformation thereby potentially affecting function, stability, efficacy, purity, and immunogenicity.[15-23]

Deamidation is a nonenzymatic, spontaneous chemical reaction that occurs via acid- and base- catalyzed pathways. In the base-catalyzed pathway, the backbone amide nitrogen on the C-terminal side of asparagine is deprotonated by OH^- in the solvent, as shown in Scheme 1. The nucleophilic attack of the resulting amidate anion on the carbonyl carbon of the asparagine side chain forms the succinimide cyclic intermediate.[24-27] The formation of the succinimide intermediate is the rate-determining step of the deamidation reaction.[24,26] The hydrolysis of the succinimide intermediate forms a mixture of isoaspartate and aspartate products in a ratio of approximately 3:1, respectively.[24,28] In addition, the resulting isoaspartate and aspartate products can be present in both L and D

Abbreviations used: HX, hydrogen exchange; HX-MS, hydrogen exchange–mass spectrometry; LC-MS, liquid chromatography–mass spectrometry; MBP, maltose-binding protein; EIC, extracted ion chromatograms; TPI, triose phosphate isomerase; ETD, electron transfer dissociation.

This article contains supplementary material available from the authors by request or via the internet at https://doi.org/10.1016/j.xphs.2019.01.019.

* *Correspondence to:* David D. Weis (Telephone: +1-785-864-1377).
E-mail address: dweis@ku.edu (D.D. Weis).

https://doi.org/10.1016/j.xphs.2019.01.019
0022-3549/

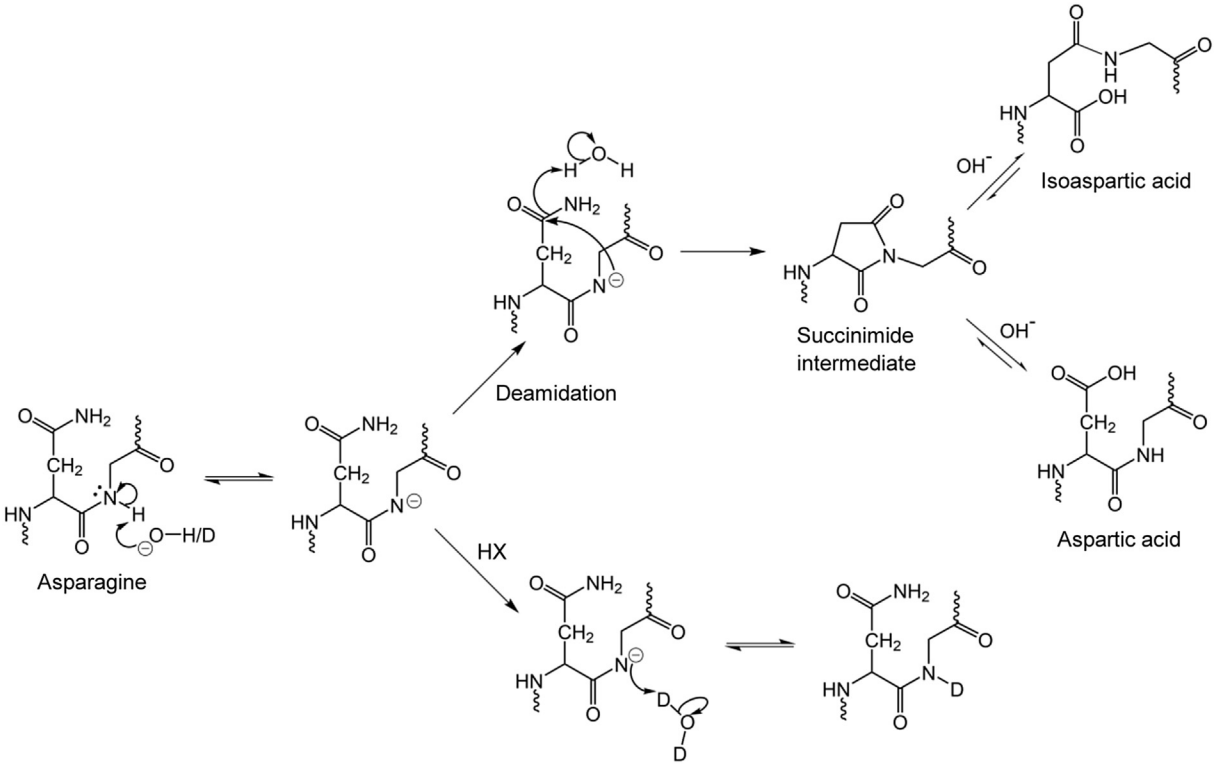

Scheme 1. Base-catalyzed deamidation and HX mechanisms at an NG motif.

isoforms.[12,29,30] Both asparagine and glutamine reactions follow the same mechanism, but the rate of glutamine deamidation is much slower than the asparagine deamidation because of the instability of the 6-membered intermediate formed in glutamine deamidation.[31] The deamidation rate is dependent on solution pH, temperature, solvent ionic strength, protein sequence, and protein higher-order structure.[32-35] Protein sequence has a stronger effect on deamidation rate than the other rate-determining factors, mostly the amino acid residue C-terminal to the asparagine residue. It has been thought that side chains with little steric hindrance enable conformational flexibility required for the intermediate formation and residues with low dipole moment stabilize the intermediate formation, thereby accelerating deamidation.[14,32] However, it is now recognized that the acidity of the amide hydrogen can be strongly influenced by backbone conformation.[36] Overall, deamidation is fastest at asparagine-glycine sites followed by asparagine-histidine and asparagine-serine sites.[14,32] In unstructured peptides at neutral pH, deamidation half-life can vary from 1 day to 1 year depending on the C-terminal side neighboring residue. Deamidation half-lives of asparagine followed by glycine, histidine, serine, alanine, and isoleucine in model pentapeptides have been reported as 1 day, 10 days, 16 days, 25 days, and 318 days, respectively, at pH 7.4, 37.0°C in 0.15 M tris-HCl. For glutamine, half-lives of unstructured peptides can extend to more than 10 years.[14,37]

It is essential to identify deamidation-prone sites early in the drug development process to eliminate candidates with deamidation liabilities, to develop stable formulations, and to re-engineer candidates with high deamidation propensity.[38] However, accurate prediction of deamidation rates in folded proteins is challenging. Compared with unstructured peptides, deamidation rates in folded proteins are much slower, ranging from days to years, because higher-order structure of proteins plays a significant role in determining deamidation rates. Higher-order structure stabilizes asparagine residues due to conformational rigidity and decreased nucleophilic reactivity of the H-bonded backbone amides.[39-44]

To determine the extent of deamidation under protein storage conditions, deamidation needs to be measured beyond the projected shelf-life, often as much as 2 years. Because such long-term stability studies are time-consuming, a common approach to identify potential deamidation sites in protein therapeutics is an accelerated stability study under stress conditions using elevated pH and temperature.[45,46] The stress conditions can increase the frequency of local and global transient unfolding, which in turn can accelerate deamidation. However, the deamidation propensities under stress conditions are different from the deamidation propensities under actual protein storage conditions.[46-48] It usually takes 3-4 weeks to complete accelerated stability-based predictions, but it is very important to limit the time required for these studies to minimize drug development time.[46] Therefore, there is a substantial need for analytical tools that can rapidly and reliably predict deamidation rates in folded proteins under long-term storage and realistic formulation conditions. Robinson et al. developed a computational method for the estimation of deamidation rates in proteins based on the sequence-controlled asparagine deamidation rates in pentapeptide models and the three-dimensional structure of proteins with well-characterized deamidations.[42,49] Sydow et al.[50] developed a computational method to predict degradation propensity of asparagine residues in the variable region of monoclonal antibodies. However, these methods require either that the three-dimensional structure of protein is known or that the structure can be accurately modeled.

Accurate prediction of deamidation rates in folded proteins requires knowledge about the protein conformation and the dynamics of amide H-bonding because the rate-determining step in the deamidation reaction mechanism involves deprotonation of a backbone amide leading to succinimide intermediate formation (see Scheme 1). These amide hydrogens contribute to the formation of the fundamental H-bonding network of protein higher-order structure.[51] Hydrogen exchange monitored by mass spectrometry (HX-MS) is a technique that measures isotopic exchange of the

protein backbone amide hydrogens. In the base-catalyzed mechanism of hydrogen exchange, an OD^- ion in the solvent abstracts the amide proton through nucleophilic attack producing an amidate ion, which is the rate-determining step of the reaction. Deprotonation is followed by the deuteration of the amidate ion (see Scheme 1) by the D_2O solvent.[52] HX reveals the conformation and the dynamics of the backbone amide hydrogens in folded proteins; the deamidation rate in folded proteins also depends on the conformation and dynamics of the amide hydrogen. Furthermore, when the reaction mechanisms of HX and deamidation are compared, the rates of both the reactions are determined by the rate of amidate ion formation, leading to the hypothesis that there is a correlation between the deamidation rates and HX rates in folded proteins. In fact, there is experimental support for this hypothesis: Phillips et al. recently found that the HX rates at the 2 adjacent amides in a mAb correlated with their deamidation rates.[53] In this study, we investigated the correlation between deamidation during long-term storage and HX to assess the potential for bottom-up HX-MS to be used as an analytical tool to rapidly predict localized long-term deamidation propensities.

Experimental

Wild-type and mutant (W169G) maltose-binding protein (MBP) were expressed in *E.* coli and purified using nickel affinity chromatography as described in Supporting Information.

Long-term and Accelerated Deamidation Studies

Samples of 20 μM wild-type and mutant MBP were prepared in 20 mM sodium phosphate, 100 mM sodium chloride, 100 μM EDTA at pH 7.0. The protein samples were sterile filtered through a 0.22 μM polyvinylidene fluoride membrane (Millipore) under sterile conditions and stored in autoclaved microcentrifuge tubes at room temperature (23 ± 2°C) in the dark. Wild-type and mutant MBP samples were collected after 1, 3, 6, 9, and 12 and 1, 3, 5, 7, 9, and 12 calendar months, respectively. For method development, deamidation was also accelerated in wild-type MBP by applying stress conditions to identify all the sites susceptible to deamidation. Wild-type MBP was buffer-exchanged by dialysis at 4°C into 50 mM tris at pH 8.5. The buffer-exchanged protein was diluted in 50 mM tris and 100 μM EDTA at pH 8.5 to prepare 50 μM protein samples that were incubated at 40°C for 4 weeks. The collected samples were flash frozen on liquid N_2 and stored at −80°C until analyzed.

Quantification of Deamidation

The extent of deamidation at asparagine sites was determined by liquid chromatography−mass spectrometry (LC-MS) analysis of the tryptic peptides of MBP, as described in more detail in the Supplementary Methods Section of Supporting Information. The relative deamidation percentage at each site was quantified using the integrated peak areas of extracted ion chromatograms (EIC) of unmodified and deamidated peptides. It has been previously shown that the peak areas of the EICs can be used for relative quantification as ionization efficiencies of deamidated and unmodified peptides are similar.[54] Deamidation percentage at each asparagine site was calculated as follows:

$$\%\ \text{deamidation} = \frac{A_d}{A_u + A_d} \times 100\%$$

where A denotes the integrated EIC peak area and the subscripts u and d denote the unmodified and deamidated peptides, respectively. The tryptic peptides selected for the quantification each contained only one deamidation site. EICs of the deamidated peptides for some asparagine sites consisted of 2 peaks resulting from the chromatographic resolution of aspartate and isoaspartate products of deamidation. For those sites, the area of both peaks was combined as deamidated products when obtaining the deamidated peptide peak area. In some cases, coelution of the unmodified and deamidated peptides was observed. In these cases, the overlap between the peaks was determined and corrected as illustrated in Supporting Figure S2 for the peptide 100-LYPFTWDAVRYNGK-113. The coelution of the unmodified and the deamidated peptides resulted in the overlap of the M+1 peak (m/z = 577.628) of the unmodified peptide with the monoisotopic peak (M) of the deamidated peptide (m/z = 577.625, see Supporting Figs. S2b and S2d). The area corresponding to the overlapping M+1 peak of the unmodified peptide was calculated by multiplying the unmodified peptide EIC peak area by the theoretical isotopic abundance of the unmodified peptide M+1 peak (99.25%) obtained using MassHunter Isotope Distribution Calculator software (Agilent, Santa Clara, CA), as shown in Supporting Figure S2e. To determine the peak area of the deamidated peptide alone, the area of the overlapping M+1 peak of the unmodified peptide was subtracted from the total peak area of the EIC of the deamidated peptide.

Deamidation Kinetics

Deamidation half-life $\left(t_{\frac{1}{2},d}\right)$ at 23 ± 2°C and pH 7.0 at each deamidation site was determined assuming first-order kinetics.[14] The deamidation rate constant at each deamidation site was obtained by linear regression of the natural log of fraction unmodified versus time for each deamidation site. Deamidation half-lives were determined from the first-order rate constant values. The error in deamidation half-life was determined by propagation of random error using the standard deviation of the slope obtained using the LINEST function in Excel.

Hydrogen Exchange−Mass Spectrometry

HX-MS measurements used robotic sample preparation followed by online pepsin digestion and LC-MS analysis of the deuterated peptic peptides, as described in more detail in the Supplementary Methods Section of Supporting Information. Samples were labeled with D_2O buffer (20 mM sodium phosphate, 100 mM sodium chloride, pD 7.0 corrected for the isotope effect[55]) at 25°C. Deuteration was normalized to 100% by labeling MBP peptic peptides obtained from offline digestion. The rate of HX was determined in terms of peptide-averaged HX half-life, $t_{\frac{1}{2},\mathrm{HX}}$; the time required to reach 50% deuteration. $t_{\frac{1}{2},\mathrm{HX}}$ values were determined by linear interpolation between the 2 HX times that spanned 50% deuteration. The error associated with the $t_{\frac{1}{2},\mathrm{HX}}$ values was determined by propagation of random errors in the slope and the intercept of the linear fit. The errors in the slope and the intercept were estimated using the standard deviations of the slope and the intercept obtained using the LINEST function in Excel.

Results

MBP was selected as a model protein for this study because it contains 21 asparagine residues; 5 of them are followed by glycine. The NG motif is the most susceptible to deamidation.[14] MBP is a 41 kDa monomeric protein with 2 distinct globular domains separated by a groove.[56] Two forms of MBP, wild-type and a mutant form (W169G), were used in the study. The mutant form is less stable than wild-type MBP, based on a lower thermal transition temperature ($\Delta T = -4.8$°C) measured by differential scanning calorimetry (see

Table 1
Tryptic Peptides Used for the Deamidation Analysis and Peptic Peptides Used for the HX Analysis of the NG and NA Sites in Both Wild-Type and Mutant MBP

Asparagine Sites	Tryptic Peptides	Peptic Peptides
N23G24	LVIWINGDK (18-26)	VIWINGDKGY (19-28)
N29G30	GYNGLAEVGK (27-36)	VIWINGDKGYNGL (19-31)
N111G112	LYPFTWDAVRYNGK (100-113)	VRYNGKL (108-114)
N184G185	YENGKYDIK (182-190)	FKYENGKY (180-187)
N238G239	GETAMTINGPWAWSNIDTSK (231-250)	TINGPWAWSN (236-245)
N196A197	DVGVDNAGAK (191-200)	VGVDNAGAKAGLTF (192-205)
N360A361	TAVINAASGR (356-365)	YAVRTAVINAASGRQTVDE (352-370)
N216A217	HMNADTDYSIAEAAFNK (214-230)	VDLIKNKHMNADTDY (207-221)
N278A279	PFVGVLSAGINAASPNK (268-284)	SAGINAASPNKEL (274-286)
N334A335	IAATMENAQK (328-337)	AKDPRIAATMENAQKGEIM (322-341)

Supporting Table S1). To investigate the potential of using HX-MS as a tool to rapidly predict deamidation rates in proteins, deamidation rates at NG and NA sites in MBP were correlated with HX rates using the shortest peptic peptides containing those asparagine sites.

Deamidation Kinetics

A long-term stability study was performed to determine deamidation rates at the asparagine sites of MBP under realistic storage conditions without temperature or pH stress. For the stability study, wild-type and mutant MBP were stored in the dark at 23 ± 2°C and pH 7.0 over 12 mo under sterile conditions. (A preliminary study indicated that deamidation was too slow to measure at 4°C, results not shown.) The intact masses of the 2 proteins were measured over the course of the study to determine if the proteins underwent any other modifications because other protein modifications can alter protein conformation affecting the protein deamidation rate. The deconvoluted masses of the 2 proteins at zero and 12 mo are shown in Supporting Figure S3. The mass of mutant MBP increased by 1.9 Da over the 12 mo, which can be attributed to the mass increase of 0.98 Da due to deamidation. For wild-type MBP, a mass increment was not observed over the 12 mo. Low abundance peaks that appeared at 41,258 Da and 41,129 Da for wild-type and mutant MBP, respectively, indicate a mass loss of 208 Da. Both MBP forms contain an N-terminal alanine preceding a hexahistidine tag; the loss of 208 Da is consistent with the hydrolysis of the first 2 N-terminal residues. In addition, 2 other peaks at 39,269 Da and 38,841 Da were observed in the mutant MBP sample after 12 mo indicating some fragmentation in the protein which could not be assigned. These 2 peaks were also detected after 7 mo of storage, but at lower abundance. The deconvoluted mass spectra did not reveal other common modifications of proteins such as oxidation that increase protein mass. Although some degradation occurred over 1 year of storage, unmodified protein remained the major form. Thus, the observed deamidation kinetics represents deamidation by the unmodified forms of the proteins. There was no substantial decrease in the soluble protein concentration in any of the protein samples over the course of storage, as determined by UV absorbance (results not shown), indicating that MBP did not form insoluble aggregates to any significant extent.

The extent of deamidation was measured by LC-MS analysis of tryptic peptides containing only one deamidation site per peptide (see Table 1). Deamidation percentage at each deamidation site was quantified using peak areas of the EICs of deamidated and unmodified tryptic peptides as described in the Experimental section. Deamidation was detected only at NG and NA sites in both protein forms during the 12 mo period; there was no deamidation detected at other asparagine sites. The asparagine residues with NG sites in MBP are N23G24, N29G30, N111G112, N184G185, N238G239, and the asparagine residues with NA sites are N196A197, N216A217, N278A279, N334A335, and N360A361. Among these sites, deamidation was only detected at N23G24, N29G30, N111G112, N184G185, N196A197, and N360A361.

Figure 1 shows the extent of deamidation at each of the deamidation sites in wild-type and mutant MBP over the 12-month period. Among the NG sites in wild-type MBP (Fig. 1a), deamidation was fastest at N184G185 and N111G112, reaching 55% and 42%, respectively, after 12 mo. There was much less deamidation at N23G24 and N29G30, which were only 6% and 4%, respectively. There was no detectable deamidation at N238G239. There was only modest deamidation at NA sites N196A197 and N360A361 (Fig. 1c) in the wild-type, reaching 7% and 1.5%, respectively. Overall, deamidation was faster in the mutant than the wild-type (Figs. 1b and 1d). In the mutant, there was extensive deamidation at both N184G185, which reached 100% deamidation, and at N111G112, which reached 55%. Deamidation was much slower at N23G24 and N29G30, which were 7.5% and 5.6%, respectively. Deamidation was not detected at N238G239 in the mutant. Deamidation was moderate at NA sites N196A197 and N360A361, reaching 17% and 7%, respectively. The deamidation half-lives $\left(t_{\frac{1}{2},d}\right)$, based on first-order kinetics,[14] obtained for each deamidation site in wild-type and mutant MBP are shown in Table 2. Faster deamidation rates in the mutant demonstrate the increased susceptibility of the mutant to deamidation due to its lower stability relative to the wild-type.

According to the X-ray crystal structure of wild-type MBP,[56] shown in Figure 2, N184G185 and N111G112, which deamidated the fastest ($t_{\frac{1}{2},d}$ of 12 ± 1 and 18 ± 2 mo, respectively), are located in solvent-exposed loop regions. N23G24 which deamidated at a moderate rate ($t_{\frac{1}{2},d}$ of 400 ± 100 mo) is located in a partially buried loop region. N29G30 which deamidated the slowest ($t_{\frac{1}{2},d}$ of 1100 ± 700 mo) is located in an α-helical region. N238G239 which did not have detectable amount of deamidation is located in a β-sheet in the core of the protein. The results of the deamidation kinetics of the NG sites demonstrate that asparagine residues in highly structured regions undergo deamidation slowly, whereas asparagine residues in less-structured regions undergo deamidation faster. Similar observations have been reported previously. Chelius et al.[57] reported, based on a study on an IgG1 mAb, that the deamidation site located in a buried β-sheet structure had a slower deamidation rate compared with the deamidation sites located on the surface of the antibody because of reduced flexibility and inaccessibility to react with water. Fukuda et al. reported that between 2 NG sites located on the surface of β_2-microglobulin, the NG site with asparagine whose side chain was involved in H-bonding deamidated much slower than another asparagine residue, which was not H-bonded. This nonhydrogen-bonded asparagine was also located in an environment enhancing the electrophilicity of the asparagine side chain and the nucleophilicity of the amide nitrogen.[58]

Considering the NA sites, the NA sites which are located in highly flexible regions from HX data (Table 2) underwent deamidation, whereas the NA sites in less-flexible regions did not measurably deamidate during the time of the study. As shown in Figure 2, N196A197 and N360A361, the NA sites which underwent deamidation, are located in α-helix termini with surface-exposed

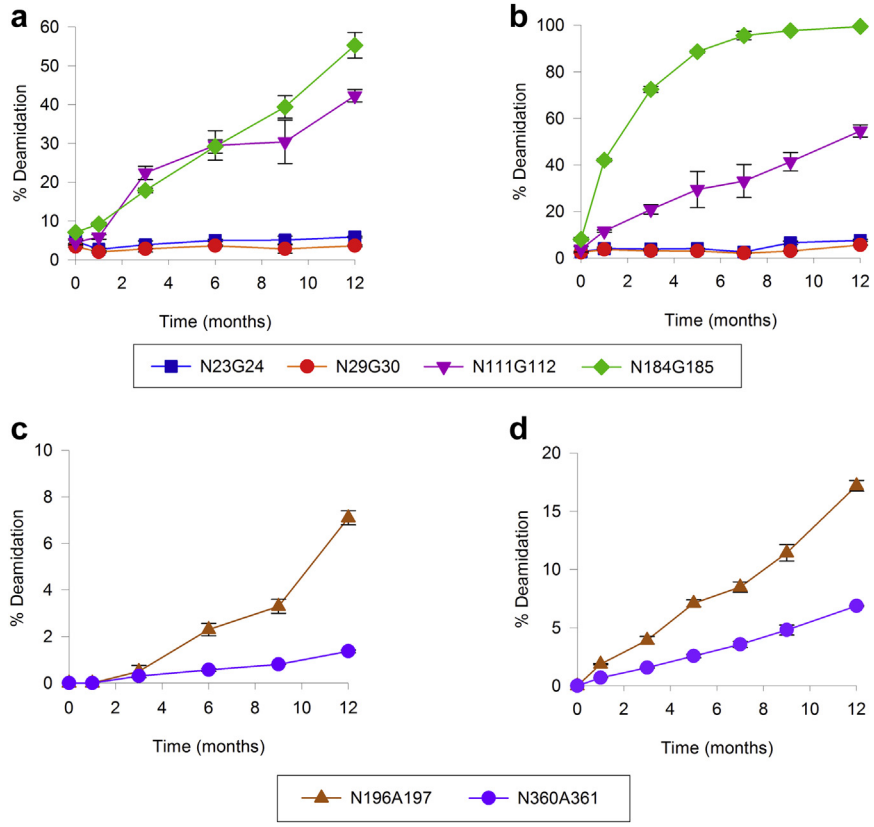

Figure 1. Extent of deamidation at each deamidation site in maltose-binding protein (MBP) in 20 mM sodium phosphate, 100 mM sodium chloride, and 100 μM EDTA, at pH 7.0 at 23 ± 2°C in the dark. (a) NG sites in wild-type MBP, (b) NG sites in mutant MBP, (c) NA sites in wild-type MBP, and (d) NA sites in mutant MBP.

asparagine side chains. N216A217 and N278A279 sites, which did not undergo deamidation, are located in loop regions. N216A217 has a partially surface-exposed asparagine side chain, N278A279 site is not on the surface, thus the apparent absence of deamidation at N216A217 is not consistent with a simple structural interpretation. N334A335, another site that did not undergo deamidation, is located in the middle of an α-helix in the core of the protein. This is consistent with previous work where between 2 unstable asparagine residues in the enzyme triosephosphate isomerase, the more solvent-accessible asparagine deamidated faster.[59]

HX Kinetics of Deamidation Sites

With peptide-level resolution, the HX rate at a specific amide cannot be determined directly. Therefore, we have used empirical $t_{\frac{1}{2},HX}$ values, the time required to reach 50% deuteration, of the shortest peptic peptides containing each deamidation site to estimate the HX rate at the deamidation sites of interest (see Table 1). The HX experiments were performed only on protein samples before storage with the goal of predicting the outcome of the long-term stability study. The wild-type and mutant MBP samples were labeled with deuterium for times ranging from 30 s to 12 h at 25°C at pD 7.0. Figure 3 shows deuterium uptake curves for the shortest peptic peptides containing the deamidation sites. Table 2 lists the $t_{\frac{1}{2},HX}$ values calculated for those peptides, obtained by linear interpolation. $t_{\frac{1}{2},HX}$ values for the peptides which reached 50% deuteration before the shortest exchange time, 30 s, cannot be estimated accurately, therefore $t_{\frac{1}{2},HX}$ values for those peptides are reported as less than 30 s. Rapid HX in these regions indicates that the protein backbone is highly dynamic.

Table 2
Deamidation Half-Lives[a] at pH 7.0 at 23 ± 2°C and HX Half-Lives at pD 7.0 Corrected for the Isotope Effect and 25°C Obtained for the NG and NA Sites in Wild-Type and Mutant MBP

Asparagine Sites	Wild-Type MBP		Mutant MBP	
	Deamidation Half-Life (mo) $t_{\frac{1}{2},d}$	HX Half-Life (s) $t_{\frac{1}{2},HX}$	Deamidation Half-Life (mo) $t_{\frac{1}{2},d}$	HX Half-Life (s) $t_{\frac{1}{2},HX}$
N23G24	400 ± 100	980 ± 60	200 ± 40	700 ± 60
N29G30	1100 ± 700	1300 ± 100	500 ± 200	600 ± 20
N111G112	18 ± 2	150 ± 10	12 ± 5	130 ± 5
N184G185	12 ± 1	<30	2.0 ± 0.5	<30
N238G239	Not detected	10,900 ± 400	Not detected	7800 ± 100
N196A197	120 ± 10	<30	50 ± 2	<30
N360A361	630 ± 30	<30	120 ± 4	<30
N216A217	Not detected	270 ± 30	Not detected	<30
N278A279	Not detected	3800 ± 400	Not detected	2600 ± 100
N334A335	Not detected	35,000 ± 900	Not detected	16,700 ± 20

[a] Deamidation half-lives were calculated from experimentally determined first-order rate constants using the data shown in Figure 1.

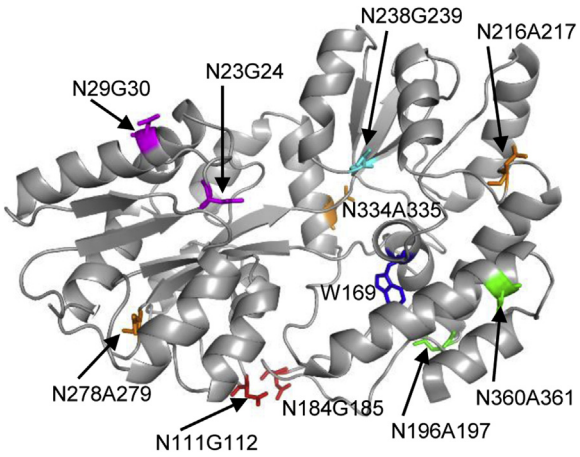

Figure 2. Locations of the NG and NA sites and the point mutation W169G on the X-ray crystal structure of wild-type MBP (PDB entry 1OMP).

In wild-type MBP, the peptic peptide containing the N238G239 site, which had no detectable deamidation, had the slowest HX, $t_{\frac{1}{2},HX} = 10900 \pm 400$ s. At the other extreme, the peptic peptide with N184G185, the NG site with the fastest deamidation rate, also had the fastest HX rate, resulting in $t_{\frac{1}{2},HX} < 30$ s. Sites with intermediate rates of deamidation also had intermediate HX rates. In the mutant, HX was generally faster at all sites, consistent with its decreased stability. Overall, the trend in HX rates is similar to the wild-type.

The 2 NA sites, N196A197 and N360A361, that deamidated at moderate rates had faster HX rates, $t_{\frac{1}{2},HX}$ values less than 30 s, in both wild-type and mutant MBP. In comparison to the deamidation rate at the NG site which had similar $t_{\frac{1}{2},HX}$ of less than 30 s, the deamidation rates of these NA sites are much slower. According to the deamidation rates of peptides reported by Robinson et al.,[14] deamidation rates at NA sites are 20-fold slower than NG sites. For the NA sites in MBP, deamidation was only detected in the regions where HX was too fast to measure and no deamidation was detected in the regions where HX rates were measurable. In other words, measurable deamidation was only observed at the most dynamic NA sites. This observation is consistent with the trends observed at NG sites among the deamidation rates and HX rates.

Correlation Between the Deamidation Rates and the HX Rates

Overall, when the deamidation kinetics $\left(t_{\frac{1}{2},d}\right)$ and HX kinetics $\left(t_{\frac{1}{2},\mathrm{HX}}\right)$ at the NG sites are compared in both protein forms, NG sites with faster deamidation rates (N184G185 and N111G112) had faster HX and NG sites with moderate and slower deamidation rates (N23G24 and N29G30) had moderate HX rates. N238G239, with no detectable deamidation, had the slowest HX. This demonstrates that the NG sites with faster deamidation rates are located in more flexible regions in the protein (indicated by faster HX rates) and the

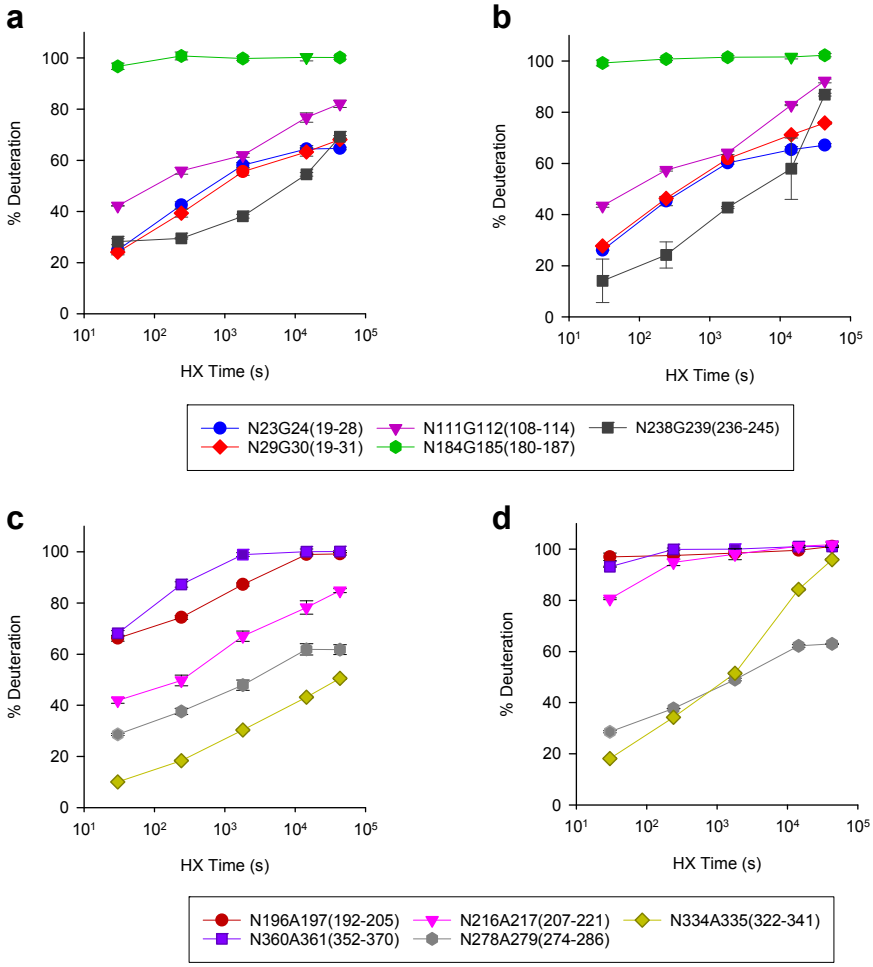

Figure 3. Hydrogen exchange kinetics at 25°C at pD 7.0 corrected for the isotope effect for the shortest peptic peptides containing each deamidation-prone site in MBP. (a) NG sites in wild-type MBP, (b) NG sites in mutant MBP, (c) NA sites in wild-type MBP, and (d) NA sites in mutant MBP.

asparagine sites with slower deamidation rates are located in less flexible or rigid regions (indicated by slower HX rates). This observation, in turn, suggests that $t_{\frac{1}{2},HX}$ values can be used to differentiate between the deamidation rates at different deamidation sites within a class of deamidation sites in a protein (e.g., NG motifs or NA motifs). Moreover, as observed between the 2 proteins states, $t_{\frac{1}{2},HX}$ values can also differentiate between the deamidation rates at a particular asparagine residue in 2 protein states with different stabilities.

To examine the correlation between deamidation and HX at the NG sites in MBP, the half-lives were correlated on a log-log plot (see Fig. 4). N184G185 and N238G239 sites were not included in the correlation analysis because HX rates of N184G185 were too fast and no deamidation was detected at N238G239. The measurable half-lives in these cases are indicated as the horizontal and vertical dashed lines in Figure 4. The results from the NA sites were not included in the correlation because either only deamidation kinetics or HX kinetics were measurable for the NA sites and also because NA sites have inherently slower deamidation rates than NG sites.[14] The square of the correlation coefficient was 0.94, demonstrating a power law relationship between deamidation rates and HX rates in MBP. The correlation can be represented as

$$t_{\frac{1}{2},d} = \frac{\left(t_{\frac{1}{2},HX}\right)^{1.8\pm0.2}}{10^{2.7\pm0.7}}$$

This correlation indicates that HX rate, based on $t_{\frac{1}{2},HX}$ values, is predictive of the deamidation rates at NG sites in MBP that have measurable HX kinetics. Thus, an initial HX analysis of MBP data yields reliable ranking of deamidation kinetics in a 1-year stability study.

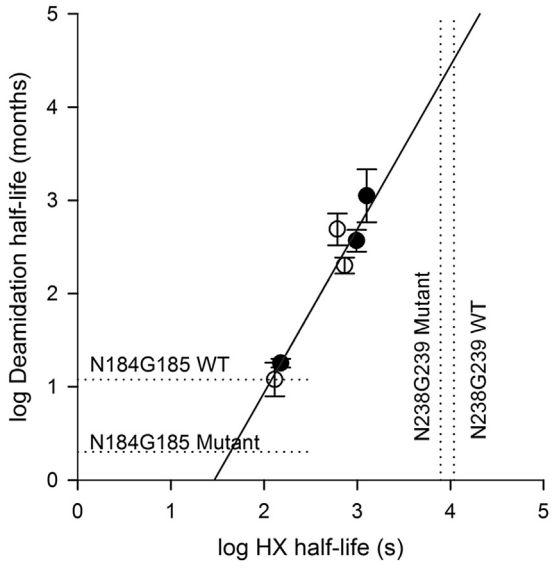

Figure 4. Correlation between HX half-life ($t_{\frac{1}{2},HX}$ in s) at 25°C at pD 7.0 corrected for the isotope effect and deamidation half-life ($t_{\frac{1}{2},d}$ in mo) at 23 ± 2°C at pH 7.0 obtained for deamidation-prone NG sites of wild-type (closed circles) and mutant (open circles) MBP, shown on a log-log plot. The R^2 value for the correlation is 0.94 and the linear fit is $y = 1.85x - 2.78$, where y denotes the base 10 log of deamidation half-life in months and x denotes the base 10 log of HX half-life in seconds. The vertical dotted lines represent the HX $t_{\frac{1}{2},HX}$ values at the N238G239 sites where deamidation was too slow to measure over 12 mo. The horizontal dotted lines represent the $t_{\frac{1}{2},d}$ of the N184G185 sites where HX was too fast for determination of $t_{\frac{1}{2},HX}$.

Discussion

Deamidation in therapeutic proteins can potentially lead to loss of efficacy or compromise safety.[13] Therefore, it is necessary to assess deamidation propensity and measure its extent in therapeutic protein candidates to select a stable protein drug candidate and to identify stabilizing conditions. Accelerated stability studies under stress conditions cannot accurately predict deamidation rates under actual drug storage conditions, thus they tend to represent a worst-case scenario. In addition, even accelerated stability studies take several weeks to complete. This makes it important and useful to identify an analytical technique that could rapidly and accurately predict deamidation rates in proteins under realistic storage conditions.

Although the asparagine sites that undergo rapid deamidation in unstructured peptides can be predicated based on amino acid sequence,[14] predicting the rates at which those sites undergo deamidation in a folded protein is not possible without understanding how higher-order structure and dynamics influence the rate. For example, in a study carried out by Gasa-Bulseco et al., NG sites located in β-sheet structure had less susceptibility to deamidation than an NN site located in a loop region, despite the fact that the NN motif has less propensity for deamidation than NG. This observation highlights the greater influence of three-dimensional structure rather than sequence in determining deamidation rates in folded proteins.[60] Although there are obvious connections between structure and deamidation in MBP, it is often the case that the precise structure of a protein of interest is not known or cannot be accurately modeled such as in the variable domains of antibodies. Therefore, gaining a better understanding of how protein conformation and backbone dynamics affect deamidation will enable more accurate predictions of protein deamidation rates based on empirical measurements. HX data reveal experimental information about how protein conformation and backbone flexibility influence the amide hydrogen bonding; the mechanism of deamidation shares the same characteristics of hydrogen exchange, leading to the hypothesis that HX could potentially be used to predict deamidation rates in proteins based on experimental observations.

Our results demonstrate a power law correlation between deamidation and HX kinetics at the NG sites in the 2 forms of MBP. This correlation suggests that HX could be used for ranking of the deamidation sites in order of their relative deamidation rates, based on peptide-averaged HX rates. Consistent with our results here, Phillips et al.[53] reported a similar observation that HX rate at the 2 amides adjacent to asparagine (residues $i + 1$ and $i + 2$, where i represents the deamidation site) correlated with the rate of deamidation. In our work, the large deviation of the exponent of power law correlation between HX and deamidation clearly indicates that there is not a linear correspondence between HX and deamidation rates. Although the mechanisms of deamidation and HX share some similar features (see Scheme 1), both reactions have complex mechanisms that defy simplified kinetic analysis. It is also likely that there is cooperativity between deamidation at different sites and other degradation pathways. In the case of NA sites, only slow deamidation was observed at the NA sites that are located in the rapidly exchanging regions. Although these sites, based on HX kinetics, are located in highly flexible regions, their deamidation occurred only at moderate rates. This can be explained by the deamidation rate dependence on protein sequence: deamidation at NA sites is approximately 20-fold slower than deamidation at NG sites.[14] At 3 other NA sites with slow HX, deamidation was undetectable even after 12 mo.

Using HX for the prediction of deamidation rates in proteins would offer a rapid method compared with both accelerated stability studies, which take several weeks, and long-term stability

studies, which can take up to 2 years. HX-based experiments and data analysis for deamidation predictions can easily be completed within 2-3 days. Although HX-MS is often considered time-consuming because of the data analysis,[61] deamidation predictions require analysis of data only for the peptides containing suspected deamidation sites. Once the peptides with deamidation sites are assigned by peptide mapping, an optimized HX-MS experiment can be completed in 1 day and HX-MS data analysis of the selected peptides can be completed in only a few hours using HX-MS data analysis software. Furthermore, HX predictions of deamidation rates can be made under realistic storage conditions rather than basing predictions on results obtained under stress conditions. In addition, as observed for wild-type and mutant MBP in this study, peptide-averaged HX rates can be used to compare relative deamidation propensities at deamidation-prone sites among similar forms of proteins such as mutants or engineered protein forms and also the same protein in different formulations in drug discovery and development. Although HX-MS cannot be a replacement for a long-term stability study, it clearly has the potential to serve as a reliable predictor of deamidation propensity that is commensurate with pharmaceutical timelines required in late discovery and early development.

The results obtained in this study are based only on 2 forms of the model protein MBP, mostly of α-helical protein. The specific correlation observed for MBP between its HX rates and deamidation rates cannot be directly applied to other proteins. Therefore, it is necessary to further explore the correlation between HX rates and deamidation rates in proteins containing other secondary structures and folds, especially the immunoglobulin fold in antibodies, and also to determine whether the correlation can be generalized or is protein specific. Usually, the time window for HX measurements ranges from tens of seconds to approximately 1 day due to experimental limitations. This time window will not capture very fast exchange requiring less than seconds and very slow exchange that can span months. This is a limitation to the application of HX that could potentially be extended using msec HX[62] and altered pH and temperature.[63-65] An additional limitation is that conventional HX-MS data are limited to peptide-level resolution where the exchange rate is averaged across the peptide and thus is not capable of achieving residue-level resolution.

The results from this study could be extended to examine the correlation between deamidation and HX rates in a wider variety of proteins including monoclonal antibodies. Furthermore, correlation between HX and other protein modifications that involve backbone dynamic changes could also be investigated to identify the potential of using HX-MS as a prediction tool for such modifications in therapeutic protein development. To improve the spatial resolution of HX data obtained in the conventional HX method, electron transfer dissociation (ETD) can be coupled with HX, which provides residue-level resolution.[66,67] With residue-level resolution, HX kinetics of the deamidation-prone residue or its neighboring residue can be obtained, which is more accurate than using peptide-averaged HX kinetics to predict deamidation propensity of a single residue or its adjacent residue as demonstrated recently with peptide-based HX-MS coupled with ETD.[53] HX coupled to ETD could be used to extend our study to investigate how the HX rate at an asparagine residue correlates with its deamidation rate and thereby to use HX as a potential tool to predict deamidation rates in proteins.

Data Sharing

Research data used in preparation of this article are available from the corresponding author on request.

Acknowledgments

An equipment loan from Agilent Technologies is gratefully acknowledged. This material is based on work supported by the National Science Foundation under Grant No. (CHE-1709176).

References

1. Walsh G. Biopharmaceutical benchmarks 2014. *Nat Biotechnol*. 2014;32(10):992-1000.
2. Lagassé HAD, Alexaki A, Simhadri VL, et al. Recent advances in (therapeutic protein) drug development. *F1000Res*. 2017;6:113.
3. Carter PJ. Potent antibody therapeutics by design. *Nat Rev Immunol*. 2006;6(5):343-357.
4. Imai K, Takaoka A. Comparing antibody and small-molecule therapies for cancer. *Nat Rev Cancer*. 2006;6(9):714-727.
5. Elvin JG, Couston RG, van der Walle CF. Therapeutic antibodies: market considerations, disease targets and bioprocessing. *Int J Pharm*. 2013;440(1):83-98.
6. Pavlou AK, Belsey MJ. The therapeutic antibodies market to 2008. *Eur J Pharm Biopharm*. 2005;59(3):389-396.
7. Aggarwal RS. What's fueling the biotech engine-2012 to 2013. *Nat Biotechnol*. 2014;32(1):32-39.
8. Liu H, Gaza-Bulseco G, Faldu D, Chumsae C, Sun J. Heterogeneity of monoclonal antibodies. *J Pharm Sci*. 2008;97(7):2426-2447.
9. Walsh G, Jefferis R. Post-translational modifications in the context of therapeutic proteins. *Nat Biotechnol*. 2006;24(10):1241-1252.
10. Gervais D. Protein deamidation in biopharmaceutical manufacture: understanding, control and impact. *J Chem Technol Biotechnol*. 2016;91(3):569-575.
11. Wang W, Singh S, Zeng DL, King K, Nema S. Antibody structure, instability, and formulation. *J Pharm Sci*. 2007;96(1):1-26.
12. Geiger T, Clarke S. Deamidation, isomerization, and racemization at asparaginyl and aspartyl residues in peptides. Succinimide-linked reactions that contribute to protein degradation. *J Biol Chem*. 1987;262(2):785-794.
13. Jenkins N, Murphy L, Tyther R. Post-translational modifications of recombinant proteins: significance for biopharmaceuticals. *Mol Biotechnol*. 2008;39(2):113-118.
14. Robinson NE, Robinson AB. Molecular clocks. *Proc Natl Acad Sci U S A*. 2001;98(3):944-949.
15. Noguchi S. Structural changes induced by the deamidation and isomerization of asparagine revealed by the crystal structure of Ustilago sphaerogena ribonuclease U2B. *Biopolymers*. 2010;93(11):1003-1010.
16. Curnis F, Longhi R, Crippa L, et al. Spontaneous formation of L-isoaspartate and gain of function in fibronectin. *J Biol Chem*. 2006;281(47):36466-36476.
17. Charache S, Fox J, McCurdy P, et al. Postsynthetic deamidation of hemoglobin Providence (beta 82 Lys replaced by Asn, Asp) and its effect on oxygen transport. *J Clin Invest*. 1977;59(4):652-658.
18. Friedman AR, Ichhpurani AK, Brown DM, et al. Degradation of growth hormone releasing factor analogs in neutral aqueous solution is related to deamidation of asparagine residues. Replacement of asparagine residues by serine stabilizes. *Int J Pept Protein Res*. 1991;37(1):14-20.
19. Solstad T, Flatmark T. Microheterogeneity of recombinant human phenylalanine hydroxylase as a result of nonenzymatic deamidations of labile amide containing amino acids. Effects on catalytic and stability properties. *Eur J Biochem*. 2000;267(20):6302-6310.
20. Mamula MJ, Gee RJ, Elliott JI, et al. Isoaspartyl post-translational modification triggers autoimmune responses to self-proteins. *J Biol Chem*. 1999;274(32):22321-22327.
21. Doyle HA, Gee RJ, Mamula MJ. Altered immunogenicity of isoaspartate containing proteins. *Autoimmunity*. 2007;40(2):131-137.
22. Moss CX, Matthews SP, Lamont DJ, Watts C. Asparagine deamidation perturbs antigen presentation on class II major histocompatibility complex molecules. *J Biol Chem*. 2005;280(18):18498-18503.
23. Shi Y, Rhodes NR, Abdolvahabi A, et al. Deamidation of asparagine to aspartate destabilizes Cu, Zn superoxide dismutase, accelerates fibrillization, and mirrors ALS-linked mutations. *J Am Chem Soc*. 2013;135(42):15897-15908.
24. Robinson NE, Robinson A. *Molecular Clocks: Deamidation of Asparaginyl and Glutaminyl Residues in Peptides and Proteins*. Cave Junction: OR: Althouse Press; 2004.
25. Catak S, Monard G, Aviyente V, Ruiz-López MF. Reaction mechanism of deamidation of asparaginyl residues in peptides: effect of solvent molecules. *J Phys Chem A*. 2006;110(27):8354-8365.
26. Capasso S, Mazzarella L, Sica F, Zagari A, Salvadori S. Kinetics and mechanism of succinimide ring formation in the deamidation process of asparagine residues. *J Chem Soc Perkin Trans*. 1993;2(4):679-682.
27. Clarke S. Propensity for spontaneous succinimide formation from aspartyl and asparaginyl residues in cellular proteins. *Int J Pept Protein Res*. 1987;30(6):808-821.
28. Reissner KJ, Aswad DW. Deamidation and isoaspartate formation in proteins: unwanted alterations or surreptitious signals? *Cell Mol Life Sci*. 2003;60(7):1281-1295.
29. Riggs DL, Gomez SV, Julian RR. Sequence and solution effects on the prevalence of d-isomers produced by deamidation. *ACS Chem Biol*. 2017;12(11):2875-2882.

30. Catak S, Monard G, Aviyente V, Ruiz-Lopez MF. Deamidation of asparagine residues: direct hydrolysis versus succinimide-mediated deamidation mechanisms. *J Phys Chem A*. 2009;113(6):1111-1120.
31. Wright HT. Nonenzymatic deamidation of asparaginyl and glutaminyl residues in proteins. *Crit Rev Biochem Mol Biol*. 1991;26(1):1-52.
32. Wakankar AA, Borchardt RT. Formulation considerations for proteins susceptible to asparagine deamidation and aspartate isomerization. *J Pharm Sci*. 2006;95(11):2321-2336.
33. Pace AL, Wong RL, Zhang YT, Kao Y-H, Wang YJ. Asparagine deamidation dependence on buffer type, pH, and temperature. *J Pharm Sci*. 2013;102(6):1712-1723.
34. Athmer L, Kindrachuk J, Georges F, Napper S. The influence of protein structure on the products emerging from succinimide hydrolysis. *J Biol Chem*. 2002;277(34):30502-30507.
35. Scotchler JW, Robinson AB. Deamidation of glutaminyl residues: dependence on pH, temperature, and ionic strength. *Anal Biochem*. 1974;59(1):319-322.
36. Radkiewicz JL, Zipse H, Clarke S, Houk KN. Accelerated racemization of aspartic acid and asparagine residues via succinimide Intermediates: an ab initio theoretical exploration of mechanism. *J Am Chem Soc*. 1996;118(38):9148-9155.
37. Robinson NE, Robinson ZW, Robinson BR, et al. Structure-dependent nonenzymatic deamidation of glutaminyl and asparaginyl pentapeptides. *J Pept Res*. 2004;63(5):426-436.
38. Yang X, Xu W, Dukleska S, et al. Developability studies before initiation of process development: improving manufacturability of monoclonal antibodies. *MAbs*. 2013;5(5):787-794.
39. Xie M. Secondary structure and protein deamidation. *J Pharm Sci*. 1999;88(1):8-13.
40. Capasso S, Salvadori S. Effect of the three-dimensional structure on the deamidation reaction of ribonuclease A. *J Pept Res*. 1999;54(5):377-382.
41. Sinha S, Zhang L, Duan S, et al. Effect of protein structure on deamidation rate in the Fc fragment of an IgG1 monoclonal antibody. *Protein Sci*. 2009;18(8):1573-1584.
42. Robinson NE, Robinson AB. Prediction of protein deamidation rates from primary and three-dimensional structure. *Proc Natl Acad Sci U S A*. 2001;98(8):4367-4372.
43. Kosky AA, Razzaq UO, Treuheit MJ, Brems DN. The effects of alpha-helix on the stability of Asn residues: deamidation rates in peptides of varying helicity. *Protein Sci*. 1999;8(11):2519-2523.
44. Wearne SJ, Creighton TE. Effect of protein conformation on rate of deamidation: ribonuclease A. *Proteins*. 1989;5(1):8-12.
45. Haberger M. Assessment of chemical modifications of sites in the CDRs of recombinant antibodies: susceptibility vs. functionality of critical quality attributes. *MAbs*. 2014;6:327-339.
46. Jarasch A, Koll H, Regula JT, Bader M, Papadimitriou A, Kettenberger H. Developability assessment during the selection of novel therapeutic antibodies. *J Pharm Sci*. 2015;104(6):1885-1898.
47. Thiagarajan G, Semple A, James JK, Cheung JK, Shameem M. A comparison of biophysical characterization techniques in predicting monoclonal antibody stability. *MAbs*. 2016;8(6):1088-1097.
48. Nowak C, J KC, S MD, et al. Forced degradation of recombinant monoclonal antibodies: a practical guide. *MAbs*. 2017;9(8):1217-1230.
49. Robinson NE. Protein deamidation. *Proc Natl Acad Sci U S A*. 2002;99(8):5283-5288.
50. Sydow JF, Lipsmeier F, Larraillet V, et al. Structure-based prediction of asparagine and aspartate degradation sites in antibody variable regions. *PLoS One*. 2014;9(6):e100736.
51. Engen JR. Analysis of protein conformation and dynamics by hydrogen/deuterium exchange MS. *Anal Chem*. 2009;81(19):7870-7875.
52. Berger A, Loewenstein A, Meiboom S. Nuclear magnetic resonance study of the protolysis and ionization of N-Methylacetamide1. *J Am Chem Soc*. 1959;81(1):62-67.
53. Phillips JJ, Buchanan A, Andrews J, et al. Rate of asparagine deamidation in a monoclonal antibody correlating with hydrogen exchange rate at adjacent downstream residues. *Anal Chem*. 2017;89(4):2361-2368.
54. Wang W, Meeler AR, Bergerud LT, Hesselberg M, Byrne M, Wu Z. Quantification and characterization of antibody deamidation by peptide mapping with mass spectrometry. *Int J Mass Spectrom*. 2012;312:107-113.
55. Glasoe PK, Long FA. Use of glass electrodes to measure acidities in deuterium oxide. *J Phys Chem*. 1960;64(1):188-190.
56. Sharff AJ, Rodseth LE, Spurlino JC, Quiocho FA. Crystallographic evidence of a large ligand-induced hinge-twist motion between the two domains of the maltodextrin binding protein involved in active transport and chemotaxis. *Biochemistry*. 1992;31(44):10657-10663.
57. Chelius D, Rehder DS, Bondarenko PV. Identification and characterization of deamidation sites in the conserved regions of human immunoglobulin gamma antibodies. *Anal Chem*. 2005;77(18):6004-6011.
58. Fukuda M, Takao T. Quantitative analysis of deamidation and isomerization in β2-microglobulin by 18O labeling. *Anal Chem*. 2012;84(23):10388-10394.
59. Ugur I, Marion A, Aviyente V, Monard G. Why does Asn71 deamidate faster than Asn15 in the enzyme triosephosphate isomerase? Answers from microsecond molecular dynamics simulation and QM/MM free energy calculations. *Biochemistry*. 2015;54(6):1429-1439.
60. Gaza-Bulseco G, Li B, Bulseco A, Liu H. Method to differentiate asn deamidation that occurred prior to and during sample preparation of a monoclonal antibody. *Anal Chem*. 2008;80(24):9491-9498.
61. Iacob RE, Engen JR. Hydrogen exchange mass spectrometry: are we out of the quicksand? *J Am Soc Mass Spectrom*. 2012;23(6):1003-1010.
62. Wilson DJ. Millisecond hydrogen exchange. In: Weis DD, ed. *Hydrogen exchange mass spectrometry of proteins: Fundamentals, methods, and applications*. Chichester: Wiley; 2016:73-92.
63. Coales SJ, E SY, Lee JE, Ma A, Morrow JA, Hamuro Y. Expansion of time window for mass spectrometric measurement of amide hydrogen/deuterium exchange reactions. *Rapid Commun Mass Spectrom*. 2010;24(24):3585-3592.
64. Walters BT, Jensen PF, Larraillet V, et al. Conformational destabilization of immunoglobulin G increases the low pH binding affinity with the neonatal Fc receptor. *J Biol Chem*. 2016;291(4):1817-1825.
65. Hamuro Y. Determination of equine cytochrome c backbone amide hydrogen/deuterium exchange rates by mass spectrometry using a wider time window and isotope envelope. *J Am Soc Mass Spectrom*. 2017;28(3):486-497.
66. Pan J, Zhang S, Chou A, Hardie DB, Borchers CH. Fast comparative structural characterization of intact therapeutic antibodies using hydrogen−deuterium exchange and electron transfer dissociation. *Anal Chem*. 2015;87(12):5884-5890.
67. Rand KD, Zehl M, Jensen ON, Jørgensen TJD. Protein hydrogen exchange measured at single-residue resolution by electron transfer dissociation mass spectrometry. *Anal Chem*. 2009;81(14):5577-5584.